Original scientific paper

Improved performance of nitrate extended gate field effect transistor sensor through deposition of polymer layer at various withdrawal speeds using dip coating method

Nor Farhana Abdullah[1], Robaiah Mamat[1], Akmal Mustaffa Zulhakim[1], Merlyne M De Souza[2], Azrif Manut[1] and Wan Fazlida Hanim Abdullah[1,✉]

[1]An Integrated Sensors Research Group, School of Electrical Engineering, College of Engineering Universiti Teknologi MARA, Shah Alam, 40450, Malaysia
[2]EEE Department, University of Sheffield, England, UK

Corresponding author: ✉*wanfaz@uitm.edu.my*

Abstract

In this study, a nitrate Extended Gate Field Effect Transistor (EGFET) sensor has been deposited with polyaniline (PANI) using a dip coating method by varying the withdrawal speed parameter at a range of 1 to 7 mm/s to improve the detection and stability of the sensor that uses zinc oxide (ZnO) as a sensing material, which lacks sensitivity and stability in detecting nitrate. The sensor was characterized by analysing its surface morphology, light absorption, and wettability level. The sensitivity and linearity of the sensors were evaluated using EGFET measurements, which showed that the threshold voltage changes when the sensor interacts with the analyte. The results obtained by comparing ZnO/indium tin oxide film and PANI/ZnO film show that PANI helps to improve sensor performance, and the best parameter setup to deposit PANI was at 2 mm/s withdrawal speed, resulting in a super-Nernstian response with a high sensitivity of 78.90 mV/dec and close to 1 linearity. The film showed excellent long-term stability in detecting nitrate in a 50-ppm nitrate solution, with the lowest drift rate at 0.1278 V/h. The dip coating method, using a 2 mm/s withdrawal speed, appears to be effective for fabricating PANI as a polymer layer for nitrate sensors.

Keywords
Electrochemical sensor; potentiometry; zinc oxide/polyaniline bilayer; surface wettability; nitrate monitoring

Introduction

Nitrate (NO_3^-) is one of the elements that commonly cause contaminants in water sources, originating from agricultural runoff, industrial discharge, and wastewater treatment plants [1,2]. Its presence in excess concentrations poses serious health risks to humans and aquatic ecosystems [3]. Therefore, developing accurate and sensitive sensors for detecting nitrate ions in water is paramount

for environmental monitoring and public health protection [4,5]. Electrochemical detection is a commonly used method that offers excellent detection capabilities. This method is marked by its high selectivity, rapid analysis, simple structures, and user-friendly operation [6,7]. To operate as chemical sensors, these methods employ an electrode as a transducer element in the presence of an analyte [8,9]. Potentiometric sensors are one type of electrochemical sensor that offers high usability, making them suitable for applications such as portable instruments that feature a straightforward setup, ease of sample preparation, and enhanced sensitivity or selectivity. These sensors operate based on the measurement of the potential difference between two electrodes, typically a reference electrode (RE) and sensing electrode (SE), in response to changes in nitrate ion concentration [9,10]. The potential difference developed at the boundary between the SE and the analyte is dependent on the concentration of nitrate as explained by the Nernst Equation (1) [9]:

$$E = E_0 + 2.3026 \frac{RT}{zF} \log a_{ion} .\tag{1}$$

where E is the potential measured across the electrodes, E_0 is the cell potential, R is the ideal gas constant, T is the temperature, F is Faraday's constant, z is the charge of the ion of interest, and a_{ion} is the ion activity [9,11]. The extended gate field effect transistor (EGFET) is a type of potentiometric transistor that isolates the field effect transistor from its surrounding chemical environment, providing several advantages [12]. These advantages include easy characterization through simple connections at low cost, minimizing interference from light and temperature, and long-term stability under various environmental conditions [13,14]. Several studies have utilized EGFET for nitrate detection on various sensing electrodes. A.B. Rosli *et. al.* [14] developed a bilayer of polymer and metal oxide nitrate EGFET sensor using a spin coating and chemical bath deposition (CBD) method. This resulted in a nitrate sensor with sensitivities of 3.9 and 59.8 mV/dec and linearity of 0.92919 and 0.98414, respectively, at nitrate concentrations ranging from 0 to 100 ppm.

Several materials are capable of detecting nitrates, including metal oxide, conductive polymer, gold, and nanoparticles. Among these materials, zinc oxide (ZnO) is considered to be one of the best options due to its biocompatibility and ease of fabrication of nanostructures [15], which provide a high surface-to-volume ratio and fast electron communication, resulting in excellent sensing performance [16-18]. However, ZnO has low stability in detection since its detection can be interfered with by other substances, such as water [19,20]. Therefore, a polymer layer is needed to improve the performance of ZnO detection [21-23].

Polyaniline (PANI) is a polymer membrane that has excellent properties for electrical applications, such as high conductivity polymer and electrical activity, which can enhance the performance of sensors [24,25]. Due to its properties, PANI offers excellent environmental stability and is easy to fabricate. It can also be easily doped with various acids and dopants. PANI can behave as both hydrophilic and hydrophobic, which affects its response to the wettability of the liquid and solid surfaces [26]. Therefore, PANI shows potential in nitrate application. For example, Kamarozaman *et al.* [27] fabricated bilayer PANI-TiO₂ sensors using the spin coating method, resulting in a sensitivity of 19.6 mV/dec, linearity of 0.8972 in nitrate concentration from 10 to 30 ppm, and long stability in response. The dip coating method is a widely used for applying films or coatings onto substrates. This process involves several parameters that control the thickness of the coating layer [28,29]. The thickness of the layer can influence the functionality of sensors as it alters the amount of composition on the surface of the film [30].

Table 1 compares potentiometric nitrate sensor sensing electrodes using different polymer membranes and sensing materials. Most works utilize spin coating as the fabrication technique,

while this work employs dip coating. Among the studies, those using spin-coated membranes exhibit low sensitivity, with detection ranges mostly spanning lower nitrate concentrations, which contrasts with this work that uses a dip-coated PANI/ZnO film, achieving the highest sensitivity and operating in a higher concentration range, indicating improved response for elevated nitrate levels.

Table 1. *Comparison of polymer membrane layer, sensing material and sensitivity for potentiometric nitrate sensor (reference electrode Ag/AgCl)*

Fabrication method	Polymer membrane	Sensing material	Sensitivity, mV/dec	Range of nitrate solution concentration, ppm	Ref.
Spin coating	Polyvinylpyrrolidone	Zinc oxide	38.90	0 - 100	[14]
Spin coating	Polyvinylpyrrolidone	Tantalum pentoxide	24.40	0 - 100	[11]
Spin coating	PANI	Titanium dioxide	19.60	10 - 30	[27]
Dip coating	PANI	Zinc oxide	78.90	50 - 250	This work

The goal of this work is to enhance the sensitivity of the ZnO/ITO film, consisting of a ZnO layer deposited on an indium tin oxide (ITO) substrate as SE for detecting nitrate ions. This was achieved by adding a PANI layer using the dip coating method while varying the withdrawal speed from 1 to 7 mm/s. The study focused on comparing the sensing performance of the ZnO/ITO film with the PANI/ZnO bilayer film for detecting nitrate ions. All samples were tested for nitrate sensing capabilities, sensitivity, and response time using an EGFET measurement setup.

Experimental

Dip coating method

The polymer studied is PANI, which was prepared for 30 mL by mixing 0.4 g of PANI (emeraldine base) powder ($[C_6H4_NH]_2[C_6H_4N]_2$) with 29.6 mL of 99.8 % N, N-Dimethylformamide (DMF), both chemical purchased from Sigma-Aldrich (St. Louis, United States). The mixture was stirred at 350 rpm for 20 minutes using a magnetic stirrer to ensure proper dilution and then sonicated at a temperature of 28 °C for 30 minutes using an ultrasonic bath. Finally, the mixture was stirred again at 350 rpm for an additional hour. The PANI solution was placed in a beaker, and the ZnO/ITO film, fabricated through spin coating at 3000 rpm for uniform spreading, was clamped onto the dip coater arm for deposition before drying at 150 °C for 10 minutes. The dip coating process was carried out with constant parameters of down speed, 20 mm/s, dipping time, 15 s, and varied parameters of withdrawal speeds from 1 to 7 mm/s using dip coater (Ossila, Sheffield, UK). After that, the films were dried on a hot plate at 100 °C for 10 minutes, as shown in Figure 1, and labelled as PANI/ZnO film.

Sensor characterization

SEM micrographs of surface morphology PANI/ZnO SE at various withdrawal speeds were captured using the Scanning Electron Microscope (SEM) (DSM 982 Leo Gemini, CAE, United States) with an operating voltage of 15 keV and a magnification of 10 to 20 k. Prior to SEM analysis, the samples were platinum coated for 1 minute using a Auto Fine Coater (JFC-16000, JEOL, USA). The optical absorbance spectra of the nanocomposite were obtained in the wavelength range of 200 to 800 nm using a UV-Vis-NIR spectrophotometer (Cary 5000 , Agilent, Carlifonia, United States). This involved comparing the intensity of light passing through a layer with the intensity passing through a blank layer. The hydrophilic properties of the polymer layer were measured using a contact angle analyser (VCA Optima, Massachusetts, USA). The contact angle was determined by gently dropping 2 µl water droplets onto the surface at low speed.
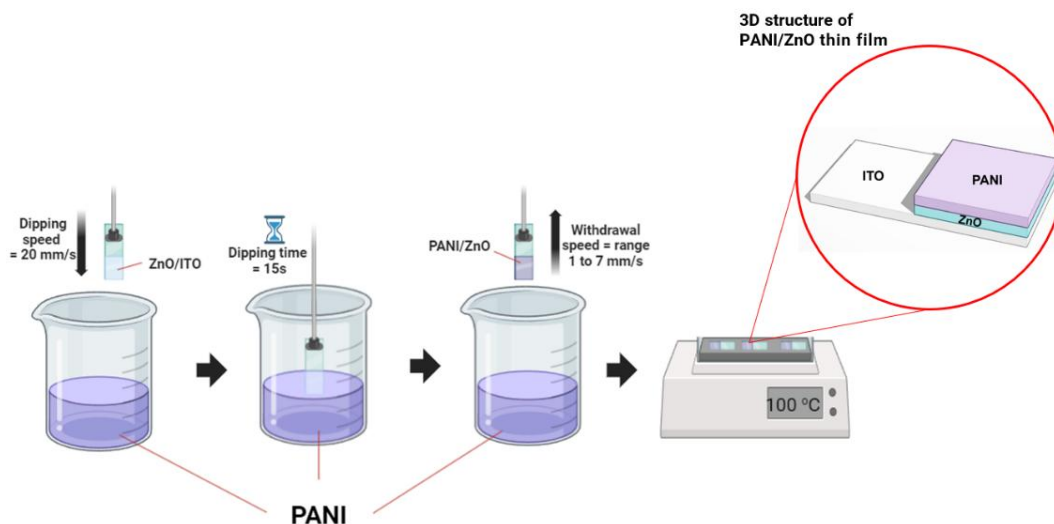
Figure 1. Dip coating method setup

Extended gate field effect transistor measurement

The sensitivity, linearity, and drift rate of PANI/ZnO film were measured silver/silver chloride (Ag/AgCl) (RE-1B, Metrohm, USA) reference electrodes (RE) in aqueous solutions through the EGFET measurement setup, as illustrated in Figure 2. The gate terminal of SE and Ag/AgCl RE has been connected to the commercialised MOSFET BS170 (onsemi, USA) to form an EGFET structure and the result of the drain current- reference voltage graph (I_D - V_{REF}) generated through B1500A Semiconductor Device Analyser (Keysight, California, USA). The gate terminal was connected to a film as an extended gate, and Ag/AgCl (RE) was immersed in nitrate solutions with a concentration at a range of 50 to 250 ppm. The sensitivity and linearity of the sensor were calculated from the slope of the graph, the reference voltage against nitrate concentration on a log scale, where V_{REF} for each sample was collected from the I_D-V_{REF} graph at 100 µA drain current for each nitrate concentration sample. The drift rate of the sensor was obtained using a commercialised MOSFET connected to the SE, while the drain and source terminals were connected to the readout integrated circuit (ROIC). The sensors were immersed in a 50-ppm nitrate solution, and V_{REF} was read by a data acquisition (DAQ) (Multifunction I/O Device, National Instrument, Texas, USA) through a graph of output voltage against time from 1 to 10 minutes.
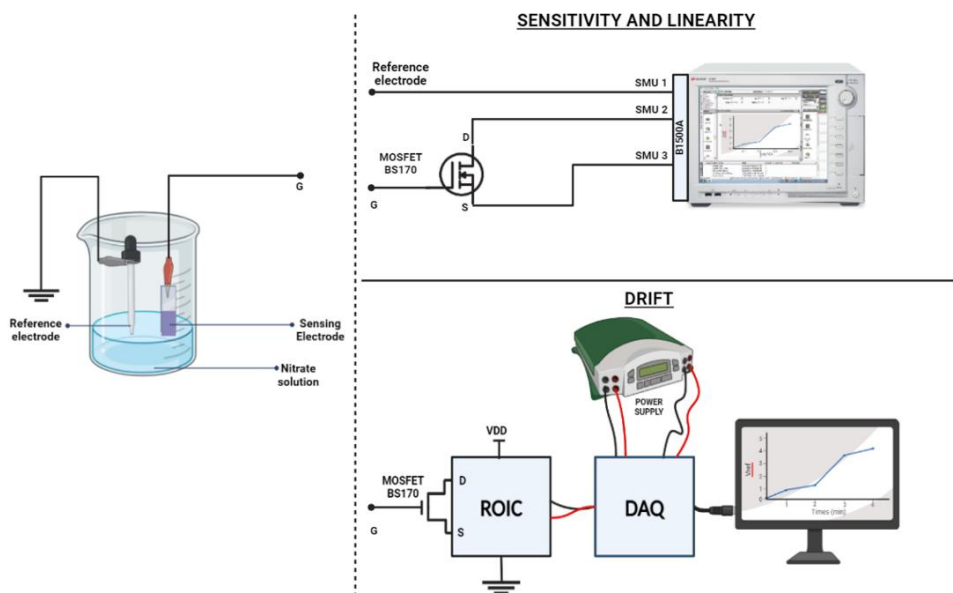

Figure 2. Sensitivity and linearity measurement setup

Results and discussion

Scanning electron microscopy

The sensing electrode surface morphology significantly influences its sensing performance. Figure 3 shows an SEM image of a 5 mm/s withdrawal speed prepared PANI/ZnO electrode. The results showed that the prepared bilayer of PANI/ZnO is not well-dispersed, which might contribute to the non-uniform surface structure of the films. Areas of non-uniformity and grain aggregation possibly result from the grafting or attachment of layers during the coating process. PANI exhibits a flaky-shaped structure [31] and non-uniform surface structure, which may be due to the weak crystalline structure and viscosity level of PANI to attach to the film during the dip coating process, while ZnO shows aggregates of spherical structure since it has been embedded in the PANI matrix [32].
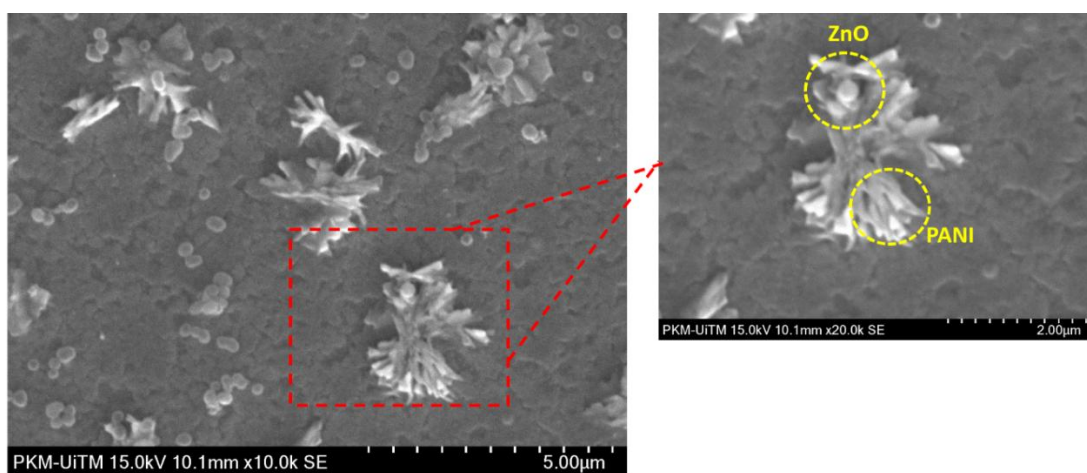

Figure 3. *SEM images of 5 mm/s PANI/ZnO film*

UV-Vis spectrophotometer

To investigate the interaction of varying withdrawal speed coated PANI with ZnO, the UV-visible absorption spectra were recorded and analysed. The UV-visible spectrum corresponding to ZnO/ITO and PANI/ZnO films is shown in Figure 4.
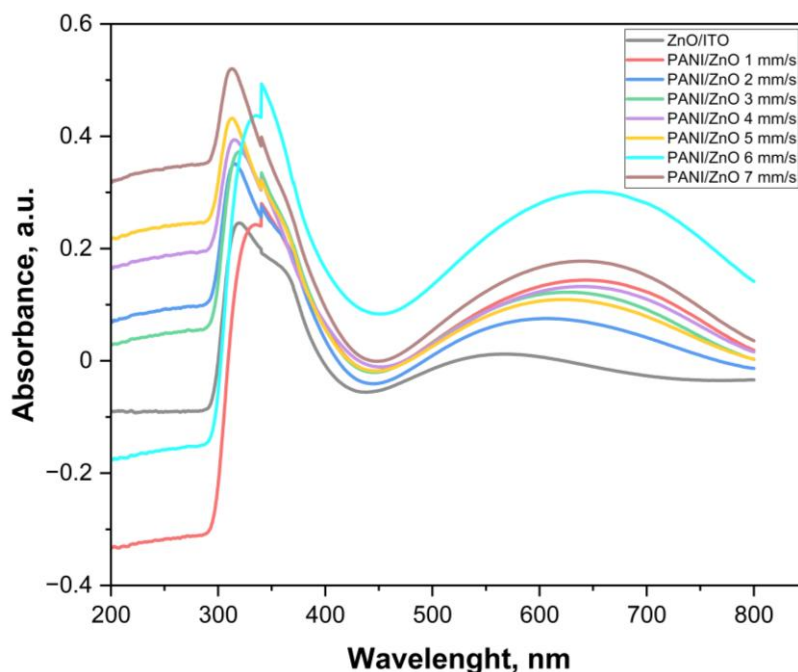

Figure 4. *Absorption spectra for ZnO/ITO film and PANI/ZnO films at different withdrawal speeds*

The film began transmitting at 300 nm and continued until 800 nm, when the plotted graph started to bend. The absorption peak of the ZnO/ITO film was at its lowest absorbance level, measuring 0.2455 a.u. at 320 nm, compared to the PANI/ZnO film, which had an additional polymer layer on top of the ZnO layer.

The absorption peak of the ZnO/ITO film was recorded as the lowest absorbance level, 0.2455 a.u. at 320 nm, compared to the PANI/ZnO film. This is due to the additional polymer layer on top of the ZnO layer. The PANI/ZnO film, with different withdrawal speeds of PANI, shows that at 7 mm/s, the highest absorbance at 0.5203 a.u. is achieved, followed by 6, 5, 4, 3, 2 and 1 mm/s, at 0.4932, 0.4322, 0.3939, 0.3730, 0.3510 and 0.2802 a.u., respectively, at the wavelength range of 300 to 400 nm. This is due to the additional layer of polymer on top of the ZnO layer, and the increase of the absorption peak is directly proportional to the withdrawal speed of dip coating. The absorbance spectra result from observing the intensity of light travelling through a layer compared to the intensity of light passing through a blank layer [33], which can be analysed through the changing thickness layer of the film.

Varying withdrawal speed will control the thickness layer, wherein this project PANI has been fabricated with withdrawal speed at a range of 1 to 7 mm/s. The film's thickness increased as the withdrawal speed increased due to the parabolic relationship between the viscosity of the PANI liquid and the rate at which the substrate was withdrawn [34]. If the coated solution has low viscosity, it will flow easily, resulting in fewer chemical elements being attached to the surface of the film during low withdrawal speeds, affecting the thickness of the layer.

Contact angle

The behaviour of films has been analysed through polymer layer response toward water contact. Films have been tested on contact angle through water layer testing. This analysis is critical to better understand the performance of film as WE. The wettability of a surface is an important factor in determining sensor interaction with its environment. The contact angle of the water droplet on the surface of the sample provides a measurement of this wettability. A high contact angle, θ <90°, indicates that the surface is hydrophobic, meaning it repels water, whereas a low contact angle, θ >90°, indicates that the surface is hydrophilic, meaning it attracts water [35,36]. The behaviour of each sample is observed based on the wettability corresponding to dropping water droplets on the surface of the sample and measuring the angle of the water droplet.

The contact angle of the ZnO/ITO film was tested to compare the wettability behaviour of surface films when a polymer layer has been added. The ZnO/ITO film contact angle test resulted in an angle of 31.90°. The PANI/ZnO films had a higher angle than ZnO/ITO, as shown in Figure 5, since ZnO lacks an affinity to water. The PANI/ZnO film for 7 mm/s withdrawal speeds of PANI showed the highest contact angle at 110.40°, followed by 6, 5, 4, 3, 2 and 1 mm/s, which were 108.50° at 1 minute, and the angle continues decreasing for 5 minutes for each film. Increasing the withdrawal speed will lead to a stronger bonding of the polymer layer on the ZnO surface. Additionally, PANI can exhibit both hydrophilic and hydrophobic properties, depending on the amount of composite attachment in the film, which influences the thickness of the coated layer [37]. A decrease in withdrawal speed will result in a hydrophobic behaviour of the polymer layer, while an increase in withdrawal speed will result in a hydrophilic behaviour [38,39].
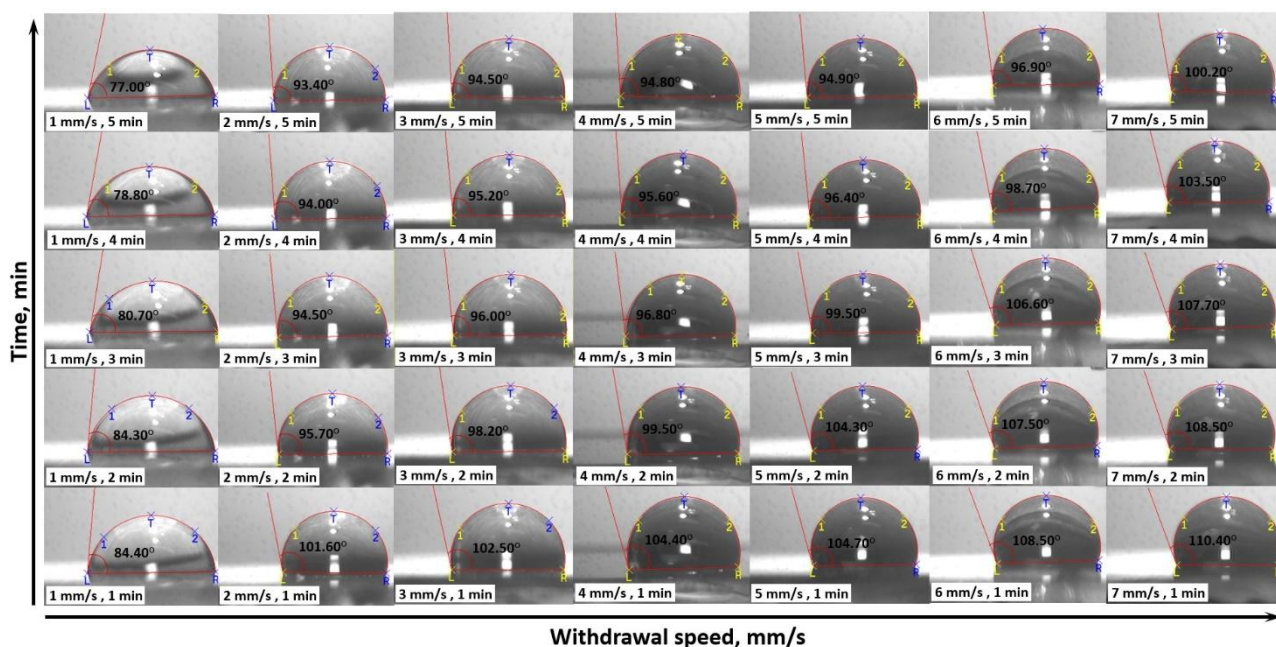
Figure 5. *Contact angles on the surface of PANI/ZnO film fabricated with different withdrawal speeds*

Sensor performance

The sensitivity and linearity of the SE were determined by analysing the current-voltage charac-teristics of the EGFET nitrate sensor. The reference electrode voltage ranged from 0 to 3 V, and the sensing electrode was measured in a nitrate solution with a concentration range of 50 to 250 ppm. The result is plotted to V_{REF} against nitrate concentration represented as a logarithmic unit (log $c_{NO_3^-}$), and then the sensitivity and linearity are determined based on the slope of the graph. The linearity value indicates the stability of sensor response follows a straight-line relationship with the logarithm of ion concentration, ensuring consistent and predictable performance. Figure 6 shows the correlation between V_{REF} and nitrate concentrations for ZnO/ITO films and PANI/ZnO films with different withdrawal speeds.

The summary of sensitivity, linearity, and drift rate results for films involving ZnO/ITO and PANI/ZnO at different withdrawal speeds has been organized in Table 2. The sensitivity of ZnO/ITO films was 137.80 mV/dec with linearity 0.5915, respectively (as shown in Figure 6a). These results indicate that the super-Nernstian nitrate response is sensitive over the Nernst response limit at room temperature, 60 mV/dec [40], and linearity is not close to one. Therefore, PANI was added to form a bilayer PANI/ZnO film to improve sensor performance. PANI/ZnO films at a withdrawal range of 1 to 7 mm/s sensitivity result in a super-Nernstian response; sensitivity increases as the withdrawal speed increases, as shown in Figure 6 (a-h). For this case, super-Nernstian response forms due to the protonation and deprotonation of PANI amine and imine groups. This leads to changes in their electrical conductivity, as PANI is a conductive polymer. This behavior causes a sensor using PANI to respond more strongly to changes in ion concentration [41]. All PANI/ZnO films produced at a 2 mm/s withdrawal speed show the best performance with a super-Nernst response sensitivity of 78.90 mV/dec and a linearity close to 1, specifically 0.9744.

The drift effect symbolizes the enduring stability of electrochemical sensors. In Figure 7, the drift curves of the ZnO/ITO film and PANI/ZnO film are shown for withdrawal speeds ranging from 1 to 7 mm/s in 50 ppm nitrate solutions over 10 minutes. The drift rate is calculated as the change in the reference voltage (ΔV_{REF}), which is defined as $\Delta V_{REF} = V_{REF}t - V_{REF}\theta$, where t is the final time and θ is the initial time of the drift measurement.
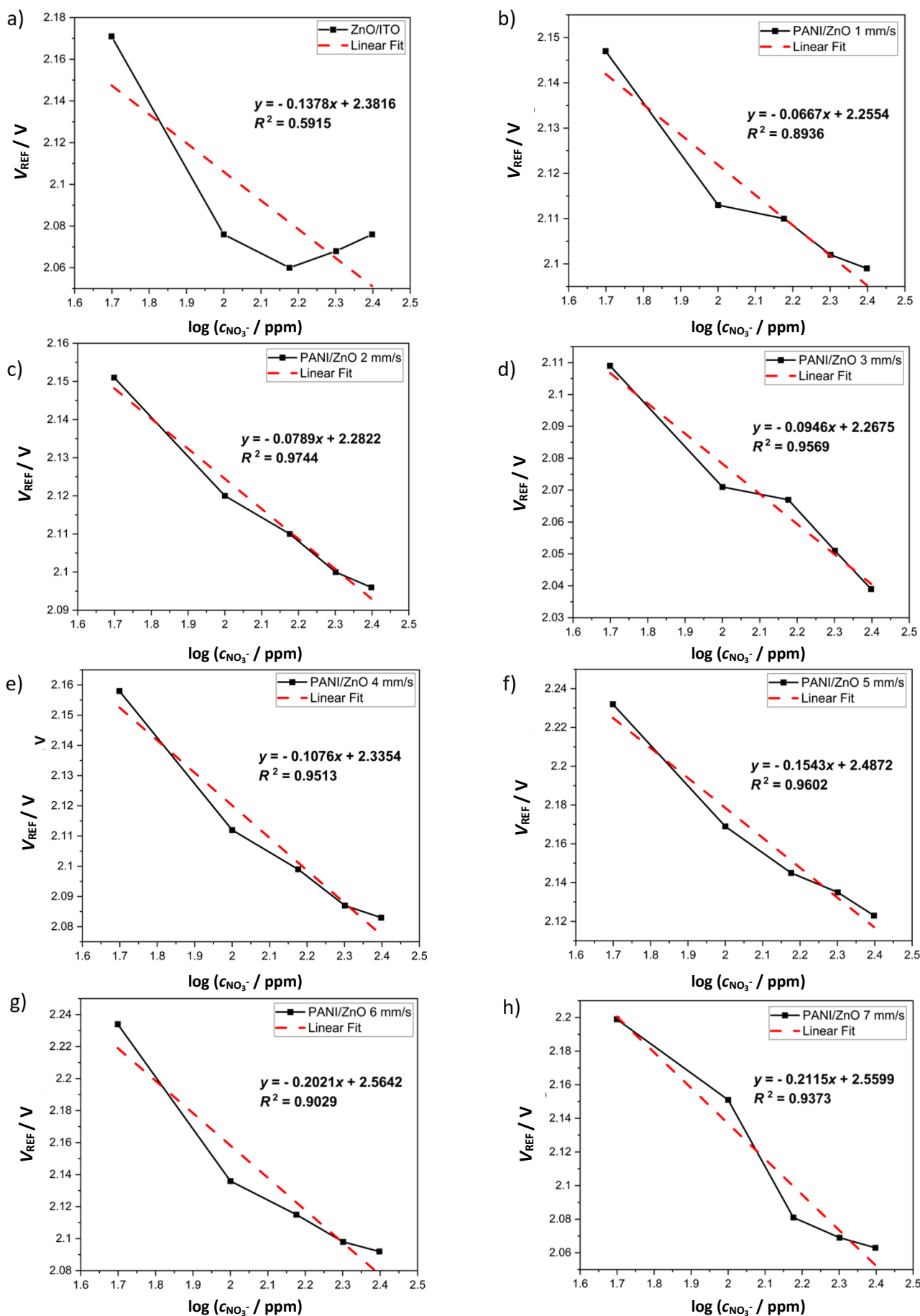
Figure 6. *Reference voltage versus nitrate concentration of (a) ZnO/ITO film and PANI/ZnO film at (b) 1, (c) 2, (d) 3, (e) 4, (f) 5, (g) 6 and (h) 7 mm/s of withdrawal speed*

The drift property is compared by calculating the drift rate ($\Delta V_{REF}/h$), where h represents the final time of the measurement in hours [27]. The drift rate of the device is shown in Table 1, with the PANI/ZnO at 2 mm/s withdrawal speed resulting in the lowest drift rate and being the most stable film working as an electrode for the nitrate EGFET sensor.
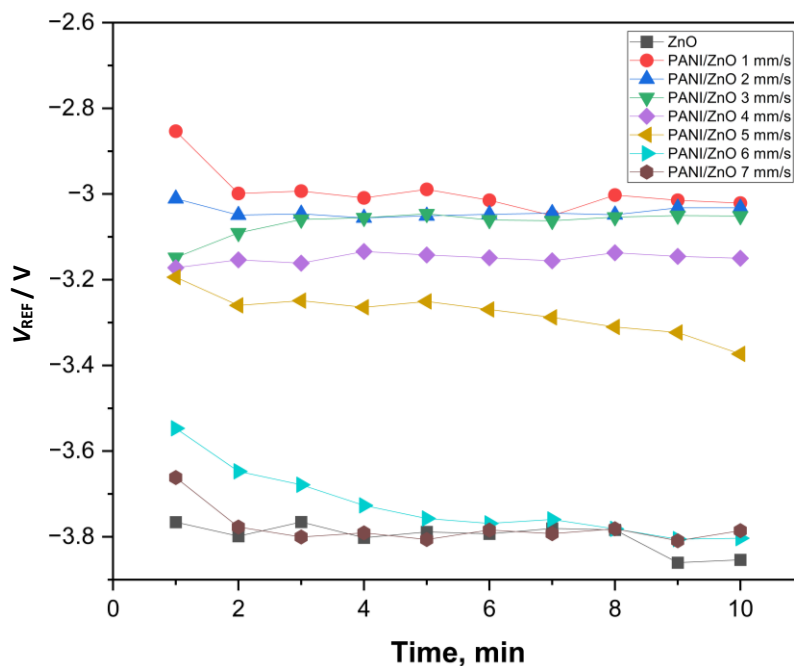

Figure 7. Drift characteristics of ZnO/ITO film and PANI/ZnO films at different withdrawal speeds

Table 2. Summary performance of ZnO/ITO film and PANI/ZnO films at different withdrawal speed thought EGFET measurement setup

Film	ZnO	Withdrawal speed of PANI fabrication layer, mm/s						
		1	2	3	4	5	6	7
Sensitivity, mV/dec	137.80	66.70	78.90	94.60	107.60	154.40	202.10	211.50
Linearity	0.5915	0.8936	0.9744	0.9569	0.9513	0.9602	0.9029	0.9373
Drift rate, V/h	0.5256	1.0056	0.1278	0.5802	0.1314	1.0758	1.5396	0.7434

Conclusions

The study examined a highly sensitive and stable PANI/ZnO film as a nitrate EGFET sensor. The nitrate EGFET sensing performance of ZnO/ITO and the varying withdrawal speed of PANI/ZnO films as the SEs were studied. The physical properties of the samples were tested to observe the behaviour and structure of PANI as a polymer layer of the film by varying the withdrawal speed, which can control the thickness of the layer and improve the film for nitrate sensing. In terms of performance, the samples were tested in 50 to 250 ppm nitrate solutions to observe sensitivity and linearity, where the best results were obtained for a withdrawal speed of 2 mm/s. The sensitivity and linearity result for 2 mm/s withdrawal speed show the super-Nernstian response and linearity close to 1. The PANI/ZnO film has shown the lowest drift rate at a withdrawal speed of 2 mm/s, indicating its strong structure and ability to react rapidly with analytes over extended periods. In conclusion, the successful use of the dip coating method to fabricate PANI, with a withdrawal speed parameter set at 2 mm/s, highlights its potential as a highly effective polymer layer for ZnO-based (ZnO/ITO) EGFET nitrate sensors.

References

[1]   M. E. E. Alahi, S. C. Mukhopadhyay, Detection methods of nitrate in water, *Sensors and Actuators A* **280** (2018) 210-221. https://doi.org/10.1016/j.sna.2018.07.026

[2]   J. Dong, J. Tang, G. Wu, Y. Xin, R. Li, Y. Li, Effective correction of dissolved organic carbon interference in nitrate detection using ultraviolet spectroscopy combined with the equivalent concentration offset method, *RSC Advances* **14** (2024) 53705379. https://doi.org/10.1039/d3ra08000e

[3]   A. N. Mallya, P. C. Ramamurthy, Design and Fabrication of a Highly Stable Polymer Carbon Nanotube Nanocomposite Chemiresistive Sensor for Nitrate Ion Detection in Water, ECS *Journal of Solid State Science and Technology* **7** (2018) Q3054Q3064. https://doi.org/10.1149/2.0081807jss

[4]   X. Chen, H. Pu, Z. Fu, X. Sui, J. Chang, J. Chen, S. Mao, Real-time and selective detection of nitrates in water using graphene-based field-effect transistor sensors, *Environmental Science: Nano* **5** (2018) 19901999. https://doi.org/10.1039/c8en00588e

[5]   R. N. Dean, E. A. Guertal and A. F. Newby, A Low-Cost Environmental Nitrate Sensor, *2020 IEEE Green Technologies Conference(GreenTech)*, Oklahoma City, OK, USA, 2020, pp. 165-170. https://doi.org/10.1109/GreenTech46478.2020.9289723

[6]   R. K. Singh, Electrochemical Sensors for Nitrate and Nitrite Detection : A Brief Review, *International Journal of All Research Education and Scientific Methods* **11** (2023) 8-12. https://doi.org/10.56025/IJARESM.2023.11623242

[7]   Z. Ren, Y. Li, A Miniaturized Electrochemical Nitrate Sensor and the Design for Its Automatic Operation Based on Distributed Model, *Mathematical Problems in Engineering* **2022** (2022) 6028110. https://doi.org/10.1155/2022/6028110

[8]   F. R. Simões, M. G. Xavier, Electrochemical Sensors, *Nanoscience and its Applications, Micro and Nano Technologies* (2017) 155-178. https://doi.org/10.1016/B978-0-323-49780-0.00006-5

[9]   C. L. Baumbauer, P. J. Goodrich, M. E. Payne, T. Anthony, C. Beckstoffer, A. Toor, W. Silver, A. C. Arias, Printed Potentiometric Nitrate Sensors for Use in Soil, *Sensors* **22** (2022) 4095. https://doi.org/10.3390/s22114095

[10] A. B. Rosli, Z. Awang, S. S. Shariffudin, S. H. Herman, Fabrication of integrated solid state electrode for extended gate-FET pH sensor, *Materials Research Express* **6** (2019) 016419. https://doi.org/10.1088/2053-1591/aae739

[11] S. B. Hashim, A. B. Rosli, Z. Zulkifli, W. Fazlida, H. Abdullah, S. H. Herman, Effect of Polymer Types on Metal Oxide Substrates as an EGFET Sensor-Based Nitrate Sensing Layers, *Science Letter* **16** (2022) 73-83. https://doi.org/10.24191/sl.v16i2.16942

[12] S. A. Pullano, C. D. Critello, I. Mahbub, N. T. Tasneem, S. Shamsir, S. K. Islam, M. Greco, A. S. Fiorillo, EGFET-based sensors for bioanalytical applications, *Sensors (Switzerland)* **18** (2018) 4042. https://doi.org/10.3390/s18114042

[13] S. Sheibani, L. Capua, S. Kamaei, S. S. A. Akbari, J. Zhang, H. Guerin, A.M. Ionescu, Extended gate field-effect-transistor for sensing cortisol stress hormone, *Communication Materials* **2** (2021) 10. https://doi.org/10.1038/s43246-020-00114-x

[14] A. B. Rosli, S. B. Hashim, R. A. Rahman, S. H. Herman, W. F. H. Abdullah, Z. Zulkifli, Correlation of ZnO Surface Morphology and Sensing Performance of EGFET Nitrate Sensor*, Journal of Mechanical Engineering* **SI 11** (2022) 65-80. https://doi.org/10.24191/jmeche.v11i1.23586

[15] R. B. M. Cross, M. M. De Souza, E. M. Sankara Narayanan, A low temperature combination method for the production of ZnO nanowires, *Nanotechnology* **16** (2005) 2188-2192. https://doi.org/10.1088/0957-4484/16/10/035

[16] S. Chaudhary, A. Umar, K.K. Bhasin, S. Baskoutas, Chemical sensing applications of ZnO nanomaterials, *Materials (Basel)* **11** (2018) 287. https://doi.org/10.3390/ma11020287

[17] F. Zhou, Y. Li, Y. Tang, F. Gao, W. Jing, Y. Du, F. Han, A novel flexible non-enzymatic electrochemical glucose sensor of excellent performance with ZnO nanorods modified on stainless steel wire sieve and stimulated via UV irradiation, *Ceramics International* **48** (2022) 14395-14405. https://doi.org/10.1016/j.ceramint.2022.01.332

[18] S. Talam, S. R. Karumuri, N. Gunnam, Synthesis, Characterization, and Spectroscopic Properties of ZnO Nanoparticles, *ISRN Nanotechnology* **2012** (2012) 372505. https://doi.org/10.5402/2012/372505

[19] P. Li, S. Yu, H. Zhang, Preparation and performance analysis of Ag/ZnO humidity sensor, *Sensors (Switzerland)* **21** (2021) 857. https://doi.org/10.3390/s21030857

[20] S. P. Amouzesh, A. A. Khodadadi, Y. Mortazavi, S. Saris, M. Asgari, MIL-100(Fe)/ZnO nano-composite sensors: An enhanced ammonia selectivity and low operating temperature, *Sensors and Actuators B* **399** (2024) 134791. https://doi.org/10.1016/j.snb.2023.134791

[21] V. S. Bhati, M. Hojamberdiev, M. Kumar, Enhanced sensing performance of ZnO nanostructures-based gas sensors: A review, *Energy Reports* **6** (2020) 46-62. https://doi.org/10.1016/j.egyr.2019.08.070

[22] Y. M. Sung, A. K. Akbar, S. Biring, C. F. Li, Y. C. Huang, S. W. Liu, The effect of ZnO preparation on the performance of inverted polymer solar cells under one sun and indoor light, *Journal Materials Chemistry C* **9** (2021) 1196-1204. https://doi.org/10.1039/D0TC04208K

[23] T. D. Kusworo, N. Aryanti, F. Dalanta, Effects of incorporating ZnO on characteristic, performance, and antifouling potential of PSf membrane for PRW treatment, *IOP Conference Series: Materials Science and Engineering* **1053** (2021) 012134. https://doi.org/10.1088/1757-899x/1053/1/012134

[24] Y. Liu, X. Cui, W. Yan, J. Wang, J. Su, L. Jin, A molecular level based parametric study of transport behavior in different polymer composite membranes for water vapor separation, *Applied Energy* **326** (2022) 120007. https://doi.org/10.1016/j.apenergy.2022.120007

[25] H. A. Khizir, T. A. H. Abbas, Hydrothermal synthesis of TiO_2 nanorods as sensing membrane for extended-gate field-effect transistor (EGFET) pH sensing applications, *Sensors and Actuators A: Physical* **333** (2022) 113231. https://doi.org/10.1016/j.sna.2021.113231

[26] M. N. Naseer, K. Dutta, A. A. Zaidi, M. Asif, A. Alqahtany, N. A. Aldossary, R. Jamil, S. H. Alyami, J. Jaafar, Research Trends in the Use of Polyaniline Membrane for Water Treatment Applications: A Scientometric Analysis, *Membranes (Basel)* **12** (2022) 777. https://doi.org/10.3390/membranes12080777

[27] N. S. Kamarozaman, N. Zainal, A. B. Rosli, M. A. Zulkefle, N. R. Nik Him, W. F. H. Abdullah, S. H. Herman, Z. Zulkifli, Highly Sensitive and Selective Sol-Gel Spin-Coated Composite TiO_2-PANI Thin Films for EGFET-pH Sensor, *Gels* **8** (2022) 690. https://doi.org/10.3390/gels8110690

[28] S. Jebali, M. Vayer, K. Belal, F. Mahut, C. Sinturel, Dip-coating deposition of nanocomposite thin films based on water-soluble polymer and silica nanoparticles, *Colloids and Surfaces A: Physicochemical and Engineering Aspects* **680** (2024) 132688. https://doi.org/10.1016/j.colsurfa.2023.132688

[29] M. Niazmand, A. Maghsoudipour, M. Alizadeh, Z. Khakpour, A. Kariminejad, Effect of dip coating parameters on microstructure and thickness of 8YSZ electrolyte coated on NiO-YSZ by sol-gel process for SOFCs applications, *Ceramics International* **48** (2022) 16091-16098. https://doi.org/10.1016/j.ceramint.2022.02.155

[30] S. F. A. Samat, M. S. P. Sarah, M. F. M. Idros, M. Rusop, Optimizing the withdrawal speed using dip coating for optical sensor, *AIP Conference Proceedings* **1963** (2018) 020018. https://doi.org/10.1063/1.5036864

[31] M. Y. Tababouchet, A. Sakri, C. Bouremel, A. Boutarfaia, Synthesis of Polyaniline-Zinc Oxide Composites: Assessment of Structural, Morphological, and Electrical Properties, *Annales de Chimie - Science des Matériaux* **47** (2023) 399-404. https://doi.org/10.18280/acsm.470606

[32] Alamgeer, M. Tahir, M. R. Sarker, S. Ali, Ibraheem, S. Hussian, S. Ali, M. Imran Khan, D. N. Khan, R. Ali, S. Mohd Said, Polyaniline/ZnO Hybrid Nanocomposite: Morphology, Spectroscopy and Optimization of ZnO Concentration for Photovoltaic Applications, *Polymers (Basel)* **15** (2023) 363. https://doi.org/10.3390/polym15020363

[33] A. Hosseini, K. Içli, M. Özenbaş, Erçelebi, Fabrication and characterization of spin-coated TiO$_2$ films, *Energy Procedia* **60** (2014) 191-198. https://doi.org/10.1016/j.egypro.2014.12.332

[34] J. Bile, M. A. Bolzinger, J. P. Valour, H. Fessi, Y. Chevalier, Antimicrobial films containing microparticles for the enhancement of long-term sustained release, *Drug Development and Industrial Pharmacy* **42** (2016) 818-824. https://doi.org/10.3109/03639045.2015.1081237

[35] G. Agrawal, Y. S. Negi, S. Pradhan, M. Dash, S. K. Samal, Wettability and contact angle of polymeric biomaterials, *Characterization of Polymeric Biomaterials* (2017) 57-81. https://doi.org/10.1016/B978-0-08-100737-2.00003-0

[36] C. W. Lee, S. J. Lee, M. Kim, Y. Kyung, K. Eom, Capacitive humidity sensor tag monitoring system using the Capacitive to Voltage Converter (CVC), *Communications in Computer and Information Science* **195** (2011) 181-189. https://doi.org/10.1007/978-3-642-24267-0_22

[37] S. Sultana, J. Matsui, M. Mitsuishi, T. Miyashita, Thickness dependence of surface wettability change by photoreactive polymer nanosheets, *Polymer Journal* **40** (2008) 953-957. https://doi.org/10.1295/polymj.PJ2008088

[38] H. Chen, H. Fan, N. Su, R. Hong, X. Lu, Highly hydrophobic polyaniline nanoparticles for anti-corrosion epoxy coatings, *Chemical Engineering Journal* **420** (2021) 130540. https://doi.org/10.1016/j.cej.2021.130540

[39] T. V. Shishkanova, P. Matějka, V. Král, I. Šeděnková, M. Trchová, J. Stejskal, Optimization of the thickness of a conducting polymer, polyaniline, deposited on the surface of poly(vinyl chloride) membranes: A new way to improve their potentiometric response, *Analytica Chimica Acta* **624** (2008) 238-246. https://doi.org/10.1016/j.aca.2008.07.001

[40] Z. Rasool, S. I. Amin, L. Majeed, I. Bashir, A. Seraj, S. Anand, Simulation-based Study of Super-Nernstian pH Sensor Based on Doping-less Tunnel-field Effect Transistor, *Silicon* **15** (2023) 4285-4296. https://doi.org/10.1007/s12633-023-02329-2

[41] Y. Tang, L. Zhong, W. Wang, Y. He, T. Han, L. Xu, X. Mo, Z. Liu, Y. Ma, Y. Bao, S. Gan, L. Niu, Recent Advances in Wearable Potentiometric pH Sensors, *Membranes (Basel)* **12** (2022) 504. https://doi.org/10.3390/membranes12050504